Inferring Florida Current volume transport from satellite altimetry

Denis L. Volkov[1,2], Ricardo Domingues[1,2,*], Christopher S. Meinen[2], Rigoberto Garcia[1,2], Molly Baringer[1,2], Gustavo Goni[2], Ryan H. Smith[2]

*presented by Ricardo Domingues

[1] University of Miami, Cooperative Institute for Marine and Atmospheric Studies - CIMAS, Miami, Florida, USA

[2] NOAA Atlantic Oceanographic and Meteorological Laboratory - AOML, Miami, Florida, USA

OSTST Meeting, October 2020

The Florida Current and Gulf Stream

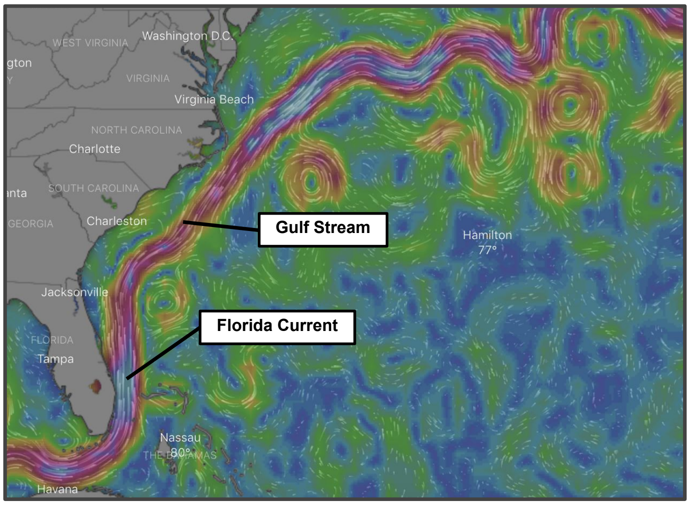

***ocean currents derived from satellite-altimetry observations for October 15, 2020**

The Florida Current (FC) is the name given to the Gulf Stream as it passes through the Straits of Florida from the southernmost Florida Keys, being one of the major conduits of heat, salt, carbon, nutrients and other properties in the subtropical North Atlantic Ocean, with profound influences on regional weather, climate, sea-level, and ecosystems. It carries the majority of the upper-ocean northward transport of warm and saline waters in the subtropical North Atlantic at this latitude, and thus accounts for the bulk of both the upper limb of the Atlantic meridional overturning circulation and the western boundary component of the subtropical gyre circulation.

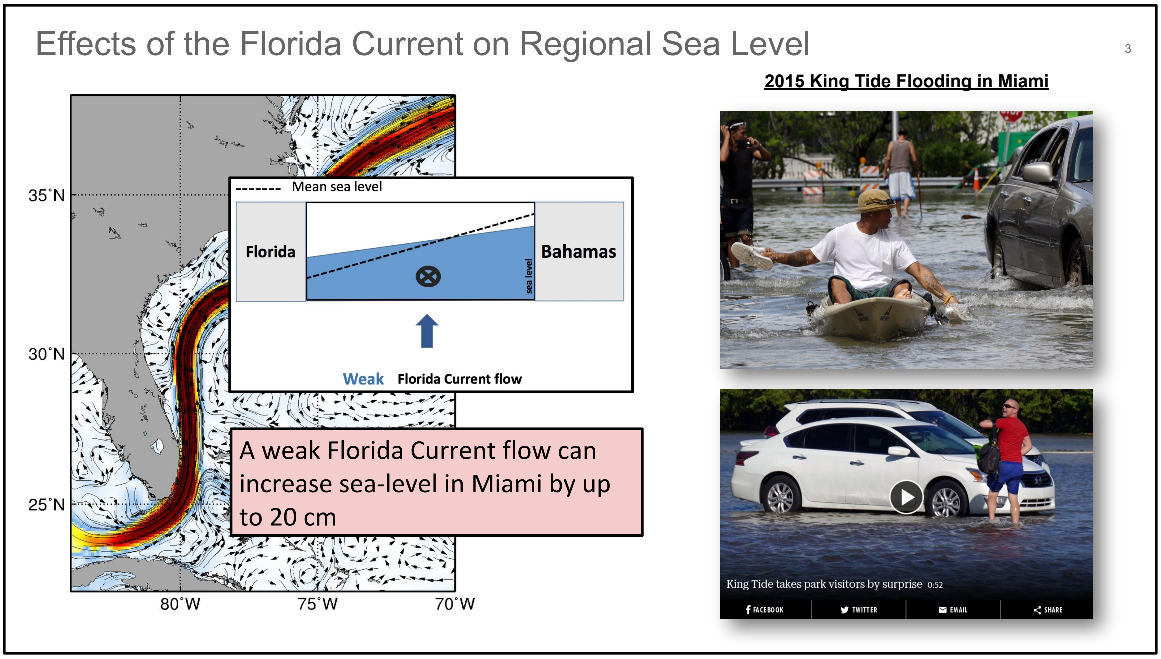

The geostrophic component of the Florida Current and Gulf Stream, for example, implies that the intensity of their flow is proportional to cross-current variations in seawater density below the sea surface, and/or to the slope of the sea level at the surface. Because of this dynamical condition, a decline of 1 Sv in the Gulf Stream transport, for example, is generally associated with a 0.5–3.0 cm sea level increase along the Northeast U.S. coast. Therefore, a weak flow by the Florida Current can increase sea-levels in Miami, and other regions along the Southeast US Coast, by up to 20 cm, which are often associated with the so called "sunny day flooding events".

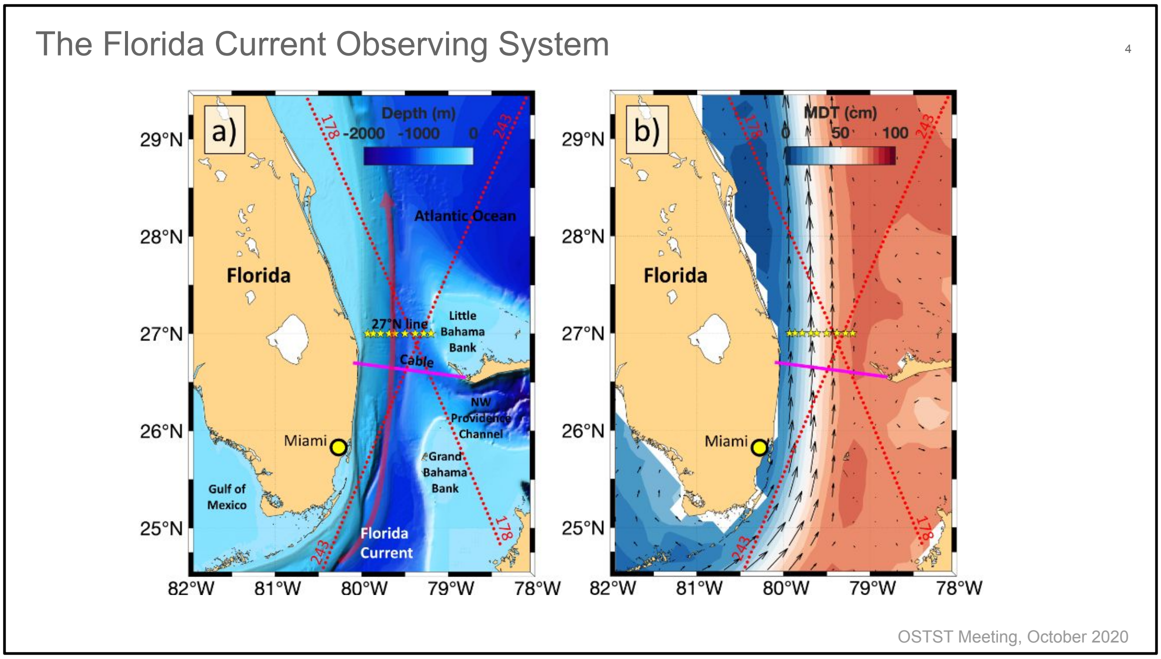

Due to its proximity to land, importance for the maritime affairs, regional sea-level, and impacts on the coupled ocean-atmosphere system, the FC is one of the most sampled western boundary currents in the world, with initial observations dating back to the late 1880s. Since 1982, the NOAA Atlantic Oceanographic and Meteorological Laboratory maintains an observing system to monitor the Florida Current, which since 1995 includes periodic hydrographic surveys.

Figure Legend. The Florida Current and its observing system components. (a) Bathymetric chart of the northern Straits of Florida: (magenta line) the submarine telephone cable between Florida and the Bahamas, (red dots) the descending track 178 and the ascending track 243 of Topex/Poseidon and Jason series satellites, (yellow stars) dropsonde and LADCP stations at 27ºN. (b) The Mean Dynamic Topography, MDT CNES-CLS18 (color), and associated mean surface geostrophic velocity (arrows). The MDT CNES-CLS18 is an estimate of the mean SSH above the geoid over the 1993-2012 period (Rio et al., 2018).

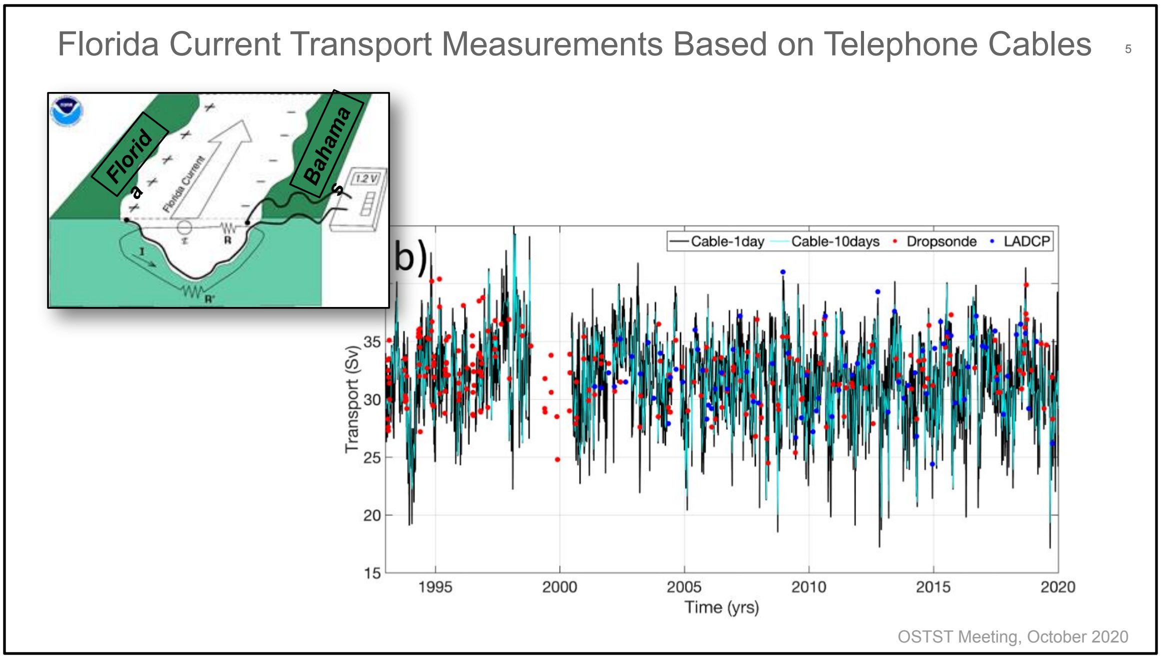

A unique component of this observing system is based on a decommissioned submarine telecommunications cable between Florida and the Bahamas, which enables a continuous measurement of the FC volume transport, T_{FC} . As of today, the daily cable time series, T_{Cable}, provides the longest quasi-continuous climate record of a boundary current in existence, and it is a critical component of the trans-basin meridional overturning circulation observing array at 26.5ºN.
The FC cable record is, therefore, a critical component of the ocean observing system, and ensuring continuity of this record into the future is of high relevance.

Overall, from the beginning of cable observations in 1982 to May 2020, the gaps constituted about 10% of the entire record. Although the cable has been the most reliable and cost-effective measurement system for T_{FC}, there have been efforts to find a suitable backup and/or replacement system that would substitute the cable during inevitable future system failures and/or future cable breaks.

Figure Legend. The Florida Current volume transport: (black) daily transport estimates, (cyan) transport estimates subsampled at 10-day intervals at the times of satellite overpasses, (red dots) transports measured with dropsonde floats, and (blue dots) transports measured with LADCP.

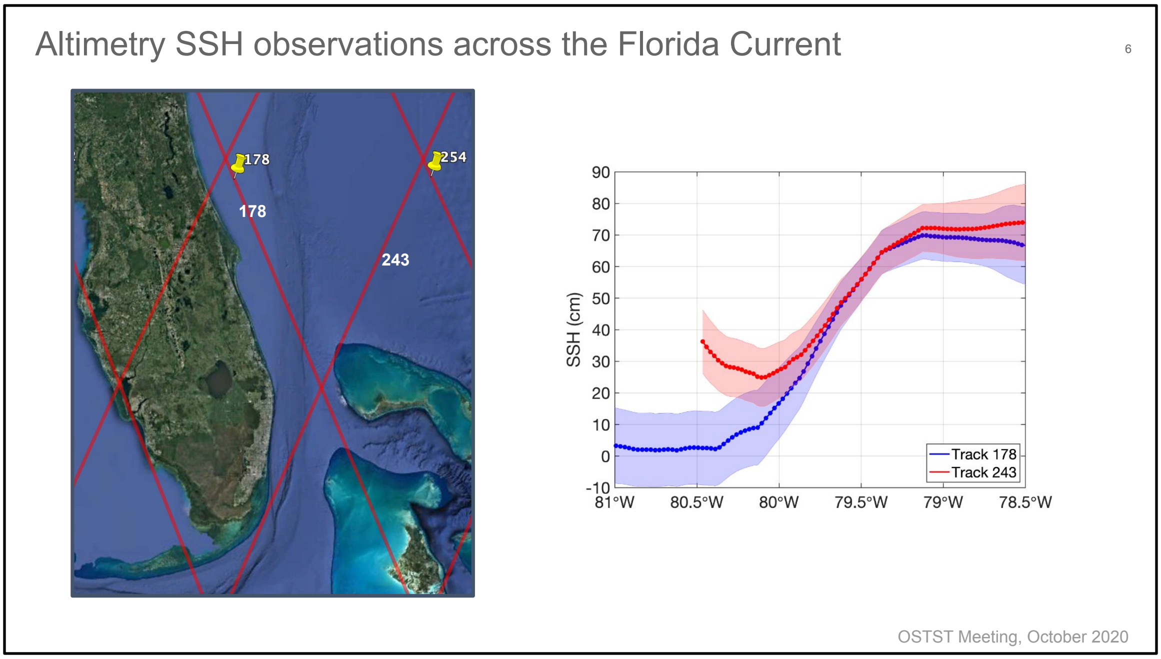

A suitable alternative is to leverage the satellite-altimetry record to derive remotely sensed estimates of the Florida Current transport. This is because, geostrophic balance dictates that a strong boundary current co-evolves with a perpendicular (cross-stream) sea level gradient, suggesting that sea level changes measured on either side of the Straits of Florida might be representative of changes in the transport.

In addition, unlike the submarine cable system, tide gauges, and shallow-water BPRs, satellite altimetry is not prone to weather conditions, and its quality is homogeneous throughout the almost 28 years of observations since 1993.
It is, therefore, possible that satellite altimetry can be used (i) to fill in the existing gaps in the cable data record during the 1993 to present altimetry period; (ii) to evaluate the consistency of cable data quality over time; and (iii) to represent a feasible future replacement for the cable system.

Figure Legend. Sea surface height (SSH) along tracks 178 (blue) and 243 (red). The dotted curves show the time-mean SSH and shading denotes ±1 standard deviation of the along-track SSH.

Objective

Derive an altimetry based record of the Florida Current transport, and evaluate its utility as a backup system for the cable measurements

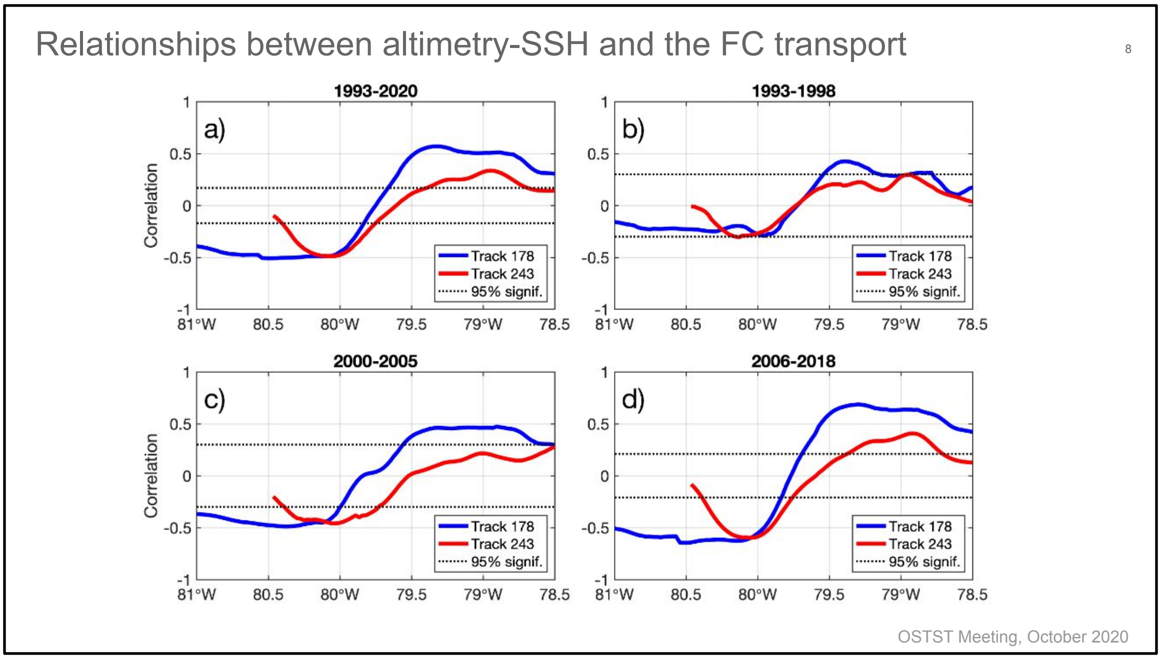

To assess the potential suitability of using altimetry observations as a potential replacement for the direct estimates measured by the FC cable, we first evaluate the correlations of along-track SSH measurements along tracks 178 and 243 and the cable-derived FC transport. Statistically significant (at 95% confidence) negative and positive correlations reaching ±0.5-0.7 are observed to the west and to the east of the FC jet, respectively. The absolute correlations obtained for track 178 are notably better than for track 243. For the entire record (1993-2020), statistically significant (at 95% confidence) correlations are observed for both the track 178 ($r = \pm0.5$-0.6) and the track 243 ($r = \pm0.3$-0.5) (Panel A). During 1993-1998, when there was the largest RMS difference (2.9 Sv) between the dropsonde and cable measurements, correlations between SSH and the cable transport were low and barely reached the 95% significance level (Panel B). During 2000-2005, correlations improved, reaching about ±0.5 for both western and eastern segments of the track 178 and for the western segment of the track 243 (Panel C). The best correlations are observed in 2006-2018 reaching ±0.6-0.7 for track 178 and ±0.4-0.6 for track 243 (Panel D). We note here that the differences in the obtained correlations reflect changes in accuracy of cable-derived estimates, since the quality of altimetry data remained stable throughout the entire 1993-2020 period. Based on the better correlation with the cable transport, hereafter we focus on SSH records only along the track 178.

Figure Legend. Correlation between the Florida Current volume transport (T_{Cable}) and the along-track SLA at tracks (blue) 178 and (red) 243 for different time intervals. The location of the tracks is shown in Fig. 1. The horizontal dotted lines show the 95% significance level for correlation.

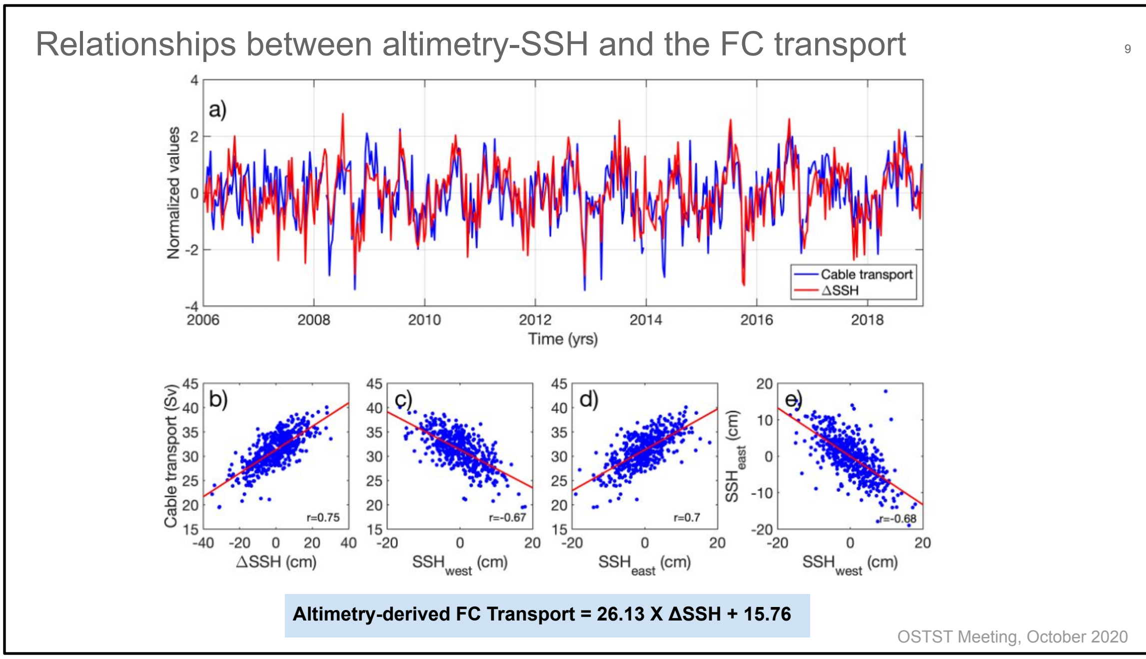

We calculate sea level differences (ΔSSH) between the eastern and western parts of the Straits of Florida: $\Delta SSH = SSH_E - SSH_W$, using the segments of maximum correlations between the cable transport and SSH (Previous Slide). The correlation between the normalized (by subtracting the mean and dividing by standard deviation) time series of T_{Cable} and ΔSSH in 2006-2018 (Panel A) is 0.75, which is significant at 95% confidence level. This means that a linear relationship between these quantities can explain about two thirds of the variance in the 10-day sampled T_{Cable}.

It is interesting to note that SSH_E and SSH_W contribute almost equally to the correlation between T_{Cable} and ΔSSH: the correlation between SSH_W and T_{Cable} is −0.67 (Panel C), and the correlation between SSH_E and T_{Cable} is 0.7 (Panel D). On average, a 1 cm change in either SSH_E or SSH_W is associated with a corresponding 0.4 Sv change in T_{Cable}, and a 1 Sv change in the FC transport is related to about a 4 cm change in ΔSSH (Panel B). Both SSH_W and SSH_E are also significantly correlated with each other ($r=-0.68$), and on average a 3 cm change in SSH_W is associated with a 2 cm change in SSH_E with the opposite sign (Fig. 7e).

These linear relationships allow us to reconstruct the FC transport strictly from altimetry observations, using the linear formula presented.

Figure Legend. (a) Time series of the daily Florida Current volume transport from the submarine cable subsampled at the days of satellite overpasses (blue) and SSH differences (ΔSSH) between the western (79-79.5ºW) and eastern (80-80.5ºW) flanks of the Florida Current (red); the time series are normalized by subtracting the 2006-2018 mean and dividing by standard deviation. (b) Scatter plot of the SSH differences and the concurrent daily T_{FC}. (c) Scatter plot of the SSH averaged over the western flank of the FC (80-80.5ºW) and the concurrent daily T_{FC}. (d) Scatter plot of the SSH averaged over the eastern flank of the FC (79-79.5ºW) and the concurrent daily T_{FC}. (e) Scatter plot of the SSH averaged over the western flank of the FC (80-80.5ºW) and over the eastern flank of the FC (79-79.5ºW). Note that in order to make scatters centered around the zero SSH, the averages of ΔSSH, SSH_{west}, and SSH_{east} over the 2006-2018 period were subtracted from the respective variables.

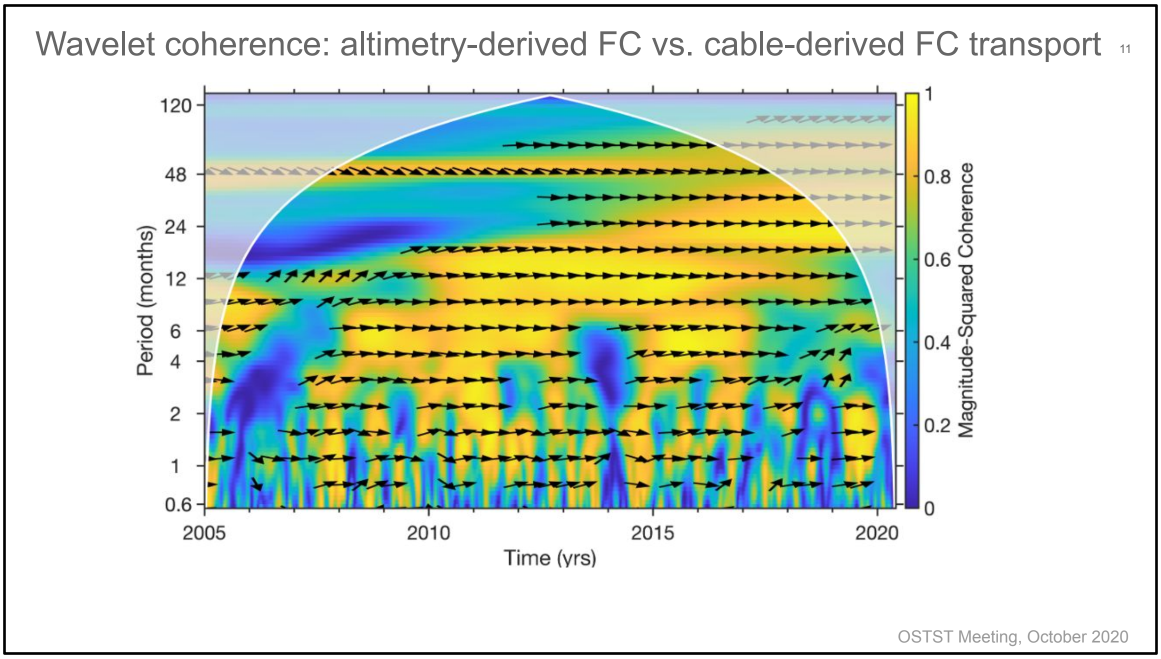

It is instructive to investigate how well the FC transport time series derived from satellite altimetry captures the variability of the daily FC transport inferred from the cable measurements at different time scales.
To account for possible nonstationarity of the signals, a magnitude-squared wavelet coherence between these transport estimates was computed using the analytic Morlet wavelet and plotted in a time-period plane. The phase of the wavelet cross-spectrum values was also computed to identify the relative lag between the input signals (arrows).

Because of the altimetry 10-day repeat cycle, the wavelet coherence has no meaningful values at periods shorter than 20 days (~0.7 months). However, there is an overall reasonable in-phase relationship between T_{Cable} and $T_{Altimetry}$ at almost all resolved scales. Particularly high coherence values (>0.8) can be seen at periods ~4-12 months, which include the seasonal cycle. There are relatively large patches of low coherence values (<0.5) in 2005-2006 and in 2013-2014 at periods shorter than 6 months, and in 2005-2011 at periods ~12-24 months. Nevertheless, it is remarkable that many high-frequency signals with periods ranging from 20 days to 4 months as well as interannual signals present in the cable data are captured by satellite altimetry.

Figure Legend. The magnitude-squared wavelet coherence between the cable- and altimetry-derived FC transport estimates. The direction of the arrows in the coherence plot corresponds to the phase lag on the unit circle, with the forward direction indicating an in-phase relationship. Frequency is plotted on a logarithmic scale. The cone of influence in the coherence plot (blurred area) indicates where edge effects occur in the coherence data.

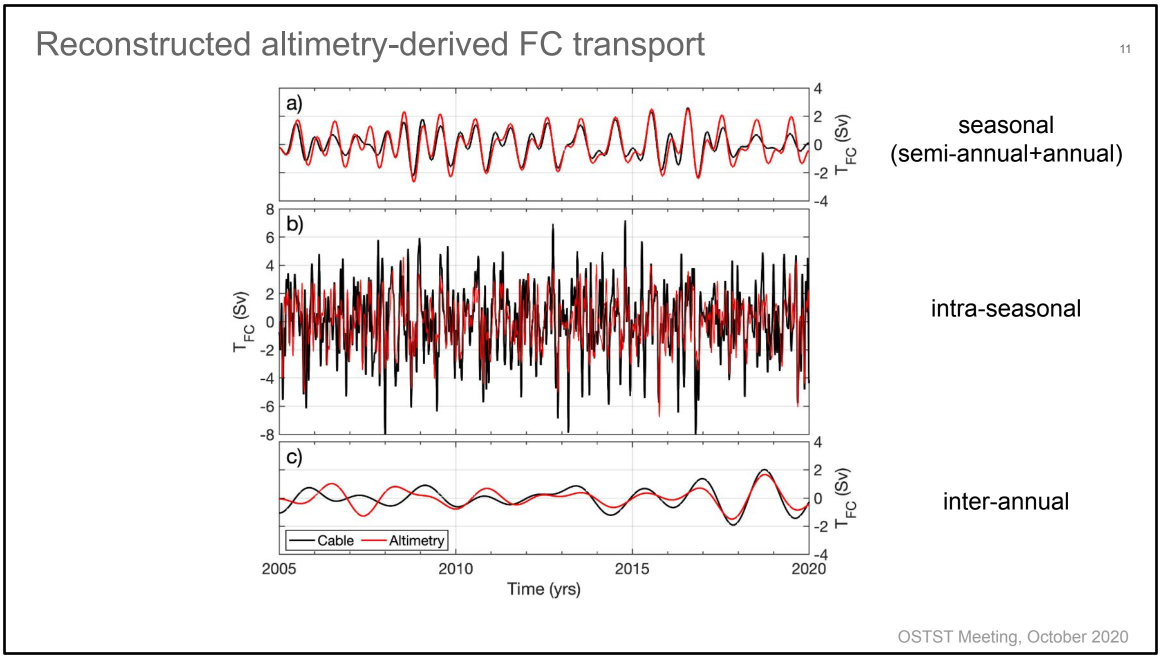

For a more detailed comparison of the individual time scales of the variability, we reconstructed T_{FC} anomalies by inverting the continuous wavelet transforms of T_{Cable} and $T_{Altimetry}$ over the following ranges of periods: 170-195 days for the semi-annual and 345-385 days for the annual components of the seasonal cycle (Panel A), 20-385 days for the intra-seasonal variability with the seasonal cycle (semi-annual + annual components) subtracted (Panel B), and greater than 540 days for the inter-annual variability (Panel C). The quantifying statistics for these scales of variability are presented in Table 4. One can see that all considered time scales of T_{Cable} variability are reasonably well reproduced by satellite altimetry measurements. The time series of T_{Cable} and $T_{Altimetry}$ associated with the seasonal, interannual, and intra-seasonal signals are significantly correlated at 95% confidence level.

Figure Legend. The FC volume transport anomalies, reconstructed by inverting the continuous wavelet transforms of (black curves) T_{Cable} and (red curves) $T_{Altimetry}$ over the range of periods associated with the following signals: (a) the seasonal cycle, obtained by summing up the annual (periods from 345 to 385 days) and semi-annual (periods from 170 to 195 days) cycles; (b) the intra-seasonal variability (periods from 20 to 385 days) with the seasonal cycle subtracted, and (c) the inter-annual variability (periods longer than 540 days).

Effects of Hurricane Forcing on Florida Current

12

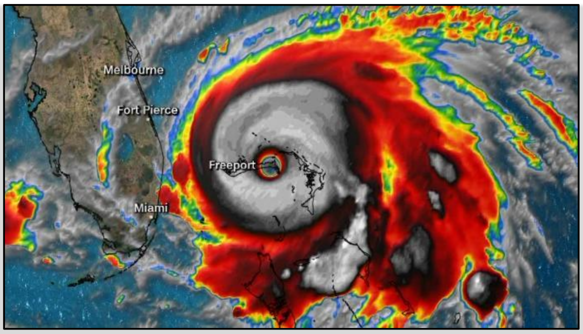

On September 2019, Hurricane Dorian caused the disruption of the Florida Current flow, causing a reduction by 47% in the flow

The low Florida Current transport contributed to the above normal coastal sea-level during Hurricane Dorian

OSTST Meeting, October 2020

Finally, one of the most important advantages of satellite altimetry over in-situ instrumentation is that it is not prone to damage from severe weather. Extreme weather events, such as tropical storms or hurricanes, can damage or destroy in-situ instruments, leading to data gaps or even to the complete termination of an observational program if the replacement of instruments is not possible or costly. Therefore, we also assessed the suitability of altimetry measurements to capture hurricane-induced changes in the Florida Current flow using observations from Hurricane Sandy (2012), and Hurricane Dorian (2019).

Figure Legend. (a-b) The FC volume transport estimates from the cable voltages (black curves), altimetry (cyan curves), dropsonde measurements (red crosses), and LADCP measurements (blue crosses) in 2012 and 2019. Hurricane Sandy was passing over the Straits of Florida on Oct. 25-30, 2012, and Hurricane Dorian was affecting the Straits of Florida on Sep. 1-6, 2019. (c-d) SSH along the track 178 around the times when (c) Hurricane Sandy and (d) Hurricane Dorian were passing over the Straits of Florida.

Effects of Hurricane Forcing on Florida Current

14

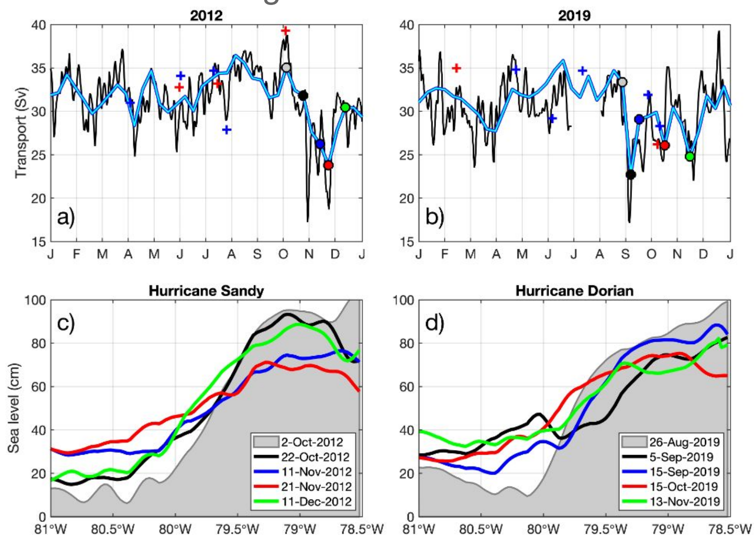

OSTST Meeting, October 2020

Analysis of observations during Hurricanes Sandy (2012) and Dorian (2019) shows that the full amplitude high-frequency variability forced by these hurricanes and captured in T_{Cable} is inevitably missed by satellites due to the 10-day sampling interval (Panels A and B). However, it is clear that satellite altimetry was able to still capture the major tendencies and the large anomalies. The passage of these hurricanes was characterized by abrupt reductions in the FC transport,$_e$ and a gradual recovery. During Hurricane Dorian, there was a satellite overpass on September 5, 2019, i.e. a day after a record minimum FC transport. On this date, the FC transport estimated from the cable and altimetry were 18.9 and 21.7 Sv, respectively (black dot in Panel B).

It is instructive to examine how the sea level slope along the satellite track 178 was changing over the dates around the passages of Hurricanes Sandy and Dorian (Fig. 13 c,d). In both cases, the strong decrease of the FC transport was associated with flattening of the along-track SSH gradient. The low transports observed by satellite altimetry on November 11 and 22, 2012 were associated with about 20-cm higher SSH to the west of the FC jet and about 20-cm lower SSH to the east of the FC jet compared to SSH observed on October 2, 2012, before the arrival of Hurricane Sandy (Panel C). Similarly, Hurricane Dorian led to a virtual destruction of the SSH gradient across the Straits of Florida, which is well reflected in the along-track SSH gradient (Panel D) associated with the lowest transport recorded by altimetry of 21.7 Sv observed on September 5, 2019. This partial destruction of the SSH gradient caused higher-than-usual sea-levels in SE Florida, which led to extensive flooding indirectly forced by the hurricane.

Figure Legend. (a-b) The FC volume transport estimates from the cable voltages (black curves), altimetry (cyan curves), dropsonde measurements (red crosses), and LADCP measurements (blue crosses) in 2012 and 2019. Hurricane Sandy was passing over the Straits of Florida on Oct. 25-30, 2012, and Hurricane Dorian was affecting the Straits of Florida on Sep. 1-6, 2019. (c-d) SSH along the track 178 around the times when (c) Hurricane Sandy and (d) Hurricane Dorian were passing over the Straits of Florida.

Conclusions

14

- Satellite altimetry is a useful tool for monitoring the Florida Current, capturing approximately 60% of the total variance observed by the cable.
- The accuracy of the altimetry-based Florida Current transport is 2.1-2.3 Sv based on comparisons with in situ measurements, slightly lower than the accuracy of the daily cable transport of 1.5 Sv.
- The altimetry-derived transport reasonably reproduces the seasonal, intra-seasonal, and inter-annual variability.
- Despite being not able to resolve high-frequency signals with periods less than 20 days, satellite altimetry provides snapshot observations of SSH across the FC that may at times capture fluctuations driven by hurricanes.
- Altimetry-based estimates can be used to fill gaps in the existing cable record, and they do represent a potential replacement system for the existing cable-based system should the latter fail.
- The Manuscript Volkov et al., Inferring Florida Current volume transport from satellite altimetry, is currently under review at the *Journal of Geophysical Research - Oceans*

Acknowledgments

The cable observations and ship section data (dropsonde and CTD/LADCP) have been supported by the U.S. NOAA Climate Program Office-Global Ocean Monitoring and Observing program via the Western Boundary Time Series (WBTS) project (FundRef number 100007298) and by the U.S. NOAA Atlantic Oceanographic and Meteorological Laboratory. The authors were supported by the WBTS project, the NOAA Climate Variability Program, and by the NOAA Atlantic Oceanographic and Meteorological Laboratory. Several authors were also supported in part under the auspices of the Cooperative Institute for Marine and Atmospheric Studies (CIMAS), a cooperative institute of the University of Miami and NOAA, cooperative agreement NA10OAR4320143.